

Chaos Control in High-Resolution Atmospheric Predictions with a Cloud-Resolving Model

Paul Krause¹
MTM/UFSC, Florianópolis, SC

Abstract. The atmospheric water cycle is dynamically unstable. The IBM prediction method is tested in high-resolution atmospheric water cycle predictions with a cloud-resolving model (CRM) with subgrid equations for viscous turbulence processes extracted from the compressible Navier-Stokes equations showing that the atmospheric water cycle has higher predictability under this method than under straightforward integrations of the CRM, both for moderate and high Reynolds numbers.

Keywords: climate change, atmospheric water cycle, cloud-resolving model, high space resolution, high Reynolds number, IBM prediction method, model error.

1 Introduction

“Climate change” is the climate transition to a new equilibrium of thermodynamical forces after disruption. More pressing than predicting the new equilibrium state is to predict how fast the transition will take place. For example: should the Amazon basin and its neighbor crop area dry up, would the change be abrupt? The atmospheric water cycle is improperly described in current climate models to figure this out. There are two major reasons for this: the cost of integrating with high space resolution a non-hydrostatic system of equations is high and the atmospheric water cycle is dynamically unstable [2, 8].

In [6] a cloud-resolving model (CRM) was presented along with a dynamical stabilization method for its dynamics. The CRM is the anelastic extension of the incompressible Navier-Stokes equations toward atmospheric convective processes [9], such as cyclones and hurricanes, coupled to subgrid equations for viscous turbulence processes derived from the compressible Navier-Stokes equations. The dynamical stabilization method, named Insertion and Brownian Motion (IBM), employs data-assimilated determining variables to control trailing variables through deterministic perturbations made in every time step (determining variables were first defined in [1]). The method was derived in [5]. The core of its derivation is Dyson’s formula, whose proof for transport operators with fields defined on a bounded open set in \mathbb{R}^n is presented in [4] (for fields in \mathbb{R}^n see [5], Appendix).

In [6] the CRM was integrated with low space resolution, namely 200km x 200km x 0.5km, using a direct numerical method (LU decomposition [7]) for solving the true pressure equations and a second-order accurate in time explicit Runge-Kutta method [7] for solving the evolution equations. Space was discretized with second-order centered finite-differences. The reaction-diffusion parameter ξ for turbulence was set to a constant and the state equation, condensation rate, radiation and surface temperature were set using the laminar pressure. The IBM prediction method was tested in this framework. In this work the CRM is integrated with high space resolution, namely 30km x

¹p.krause@ufsc.br

30km x 0.5km, using Jacobi iterations [7] for solving the numerical pressure equations ([3], eq. 4c) and the fourth-order accurate in time explicit Adams-Bashforth method [7] for solving the evolution equations. In the CRM, ξ is set to the Smagorinsky-Lilly model for eddy viscosity [10] and the state equation, condensation rate, radiation and surface temperature are set using the total pressure (i.e. the sum of the laminar and turbulent pressures). The IBM method is tested in this new framework.

The updates in the CRM are described in section 2. The high-resolution numerical treatment is described in section 3. Results for moderate and high Reynolds numbers are presented in section 4. Conclusions are drawn in section 5.

2 Model

The CRM is described in [6]. The following changes were made to it in this work:

1. The state equation $p = R\rho T$, where R is the ideal gas constant, applies to hydrostatic flows (slow motion of infinitesimal elements). For laminar flows,

$$\bar{p} = R\bar{\rho}\bar{T} \tag{1}$$

is a good approximation. Assuming

$$\bar{p} + \overset{\vee}{p} = R\bar{\rho}\bar{T} \tag{2}$$

is a good approximation for turbulent flows, where \bar{p} and $\overset{\vee}{p}$ are the laminar and turbulent pressures, the state equation, condensation rate, radiation and surface temperature are set using equation 2 instead of 1;

2. The reaction-diffusion parameter ξ for turbulence is set to the Smagorinsky-Lilly model for eddy viscosity [10]: $\xi = (C_s\Delta)^2\sqrt{s}$, where $C_s \in [0.1, 0.2]$ is the Smagorinsky constant, $\Delta = \sqrt{\Delta x^2 + \Delta y^2}$ for the horizontal value or Δz for the vertical value and

$$s = 2\left(\frac{\partial\bar{u}^2}{\partial x} + \frac{\partial\bar{v}^2}{\partial y} + \frac{\partial\bar{w}^2}{\partial z}\right) + \left(\frac{\partial\bar{u}}{\partial y} + \frac{\partial\bar{v}}{\partial x}\right)^2 + \left(\frac{\partial\bar{u}}{\partial z} + \frac{\partial\bar{w}}{\partial x}\right)^2 + \left(\frac{\partial\bar{v}}{\partial z} + \frac{\partial\bar{w}}{\partial y}\right)^2,$$

wherein \bar{u} , \bar{v} and \bar{w} are the laminar wind velocity components.

3 Numerics

The numerical pressure ([3], eq. 4c) is easier to treat and less costly to compute than the true pressure ([6], eq. 65 or 70), especially in curved domains. It is a good approximation to the true pressure for “intermediate” time step sizes, dt . The CRM is set with rotating Cartesian coordinates in a three-dimensional rectangular domain and integrated with space resolution 30km x 30km x 0.5km and reference time step size $dt = 2.5s$ using 100 Jacobi iterations for solving the numerical pressure equations and the fourth-order accurate in time explicit Adams-Bashforth method for solving the evolution equations. Space is discretized with second-order centered finite-differences. The boundary conditions are described in [6]. In this numerical framework the CRM has horizontal and vertical diffusion bounds strictly between $1 \cdot 10^7 m^2/s$ and $2 \cdot 10^7 m^2/s$ and between $1 \cdot 10^3 m^2/s$ and $2 \cdot 10^3 m^2/s$, respectively.

The IBM method is described in [6]. In this work the vertical laminar wind velocity component is not perturbed in it, only the turbulent wind velocity components and the specific humidity are perturbed, and the laminar and turbulent pressure fields are frozen within one reference time step long time intervals.

4 Results

The horizontal laminar wind velocity components and the potential temperature are set as control variables in the IBM prediction method. In practice their initial values would be data-assimilated. Here they are taken from the reference run, i.e. the run simulating the true state evolution. The global root-mean-square error plots obtained from free (no data-assimilation), insertion (straight-forward integration with initial control values taken from the reference run) and IBM runs for moderate and high Reynolds numbers are presented next. In both case studies the initial maximum and mean absolute values of the total wind velocity components in the reference run are about $u = 81\text{m/s}$, $v = 56\text{m/s}$, $w = 0.24\text{m/s}$ and $u = 12\text{m/s}$, $v = 10\text{m/s}$, $w = 0.02\text{m/s}$, respectively (the total wind velocity is the sum of the laminar and turbulent wind velocities).

4.1 Moderate Reynolds number

In this case study all the horizontal and vertical laminar viscosities are set to $2 \cdot 10^6\text{m}^2/\text{s}$ and $200\text{m}^2/\text{s}$, respectively. With ξ set to the Smagorinsky-Lilly model for viscosity the reference and free runs come out numerically stable in this framework, showing that the turbulent wind is properly balancing the laminar wind. Figure 1 shows the evolution of the condensation rate, the vertical laminar wind velocity component and the potential temperature global errors obtained from free, insertion and IBM runs with same initial state. One sees that the condensation rate has higher predictability under the IBM method than under the insertion method in this framework.

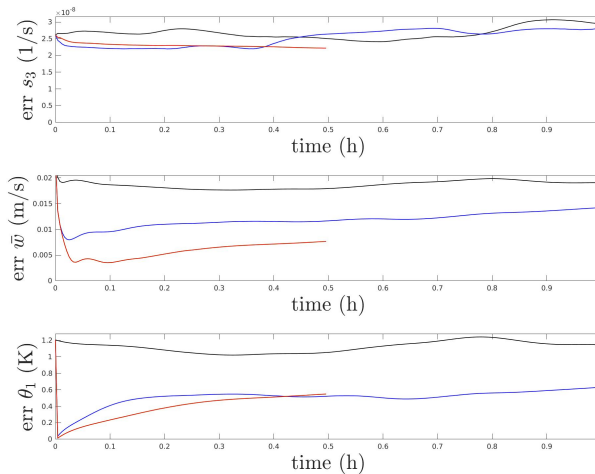


Figure 1: Global rms error plots of the condensation rate (top), the vertical laminar wind velocity component (center) and the potential temperature (bottom) obtained from free (black), insertion (blue) and IBM (red) runs at moderate Reynolds number. Source: author.

4.2 High Reynolds number

In this case study all the horizontal and vertical laminar viscosities are set to $100\text{m}^2/\text{s}$ and $0.01\text{m}^2/\text{s}$, respectively. With ξ set to the Smagorinsky-Lilly model for viscosity the reference and free runs come out numerically stable in this framework, showing that the turbulent wind is properly balancing the laminar wind. Figure 2 shows the evolution of the condensation rate, the vertical laminar wind velocity component and the potential temperature global errors obtained from free, insertion

and IBM runs with same initial state. One sees that the condensation rate has higher predictability under the IBM method than under the insertion method in this framework.

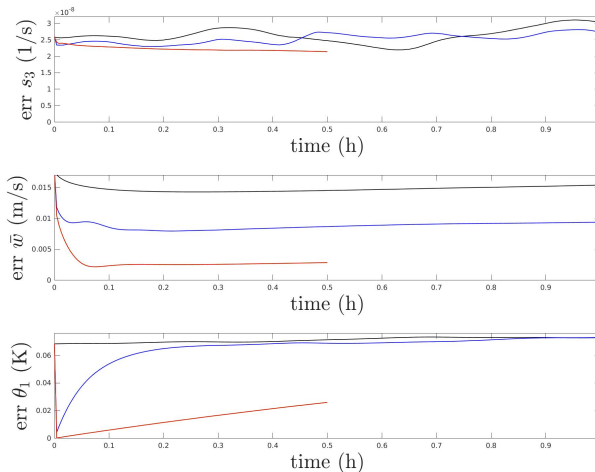


Figure 2: Global rms error plots of the condensation rate (top), the vertical laminar wind velocity component (center) and the potential temperature (bottom) obtained from free (black), insertion (blue) and IBM (red) runs at high Reynolds number. Source: author.

5 Conclusion

Nature is teeming with dynamically unstable processes that are roughly described in climate models because they are hard to predict under straightforward integrations of models. The atmospheric water cycle is an example: the condensation rate is dynamically unstable because the vertical laminar (hence the vertical total) wind velocity component and the temperature are so when the turbulent wind velocity components are strongly perturbed from their reference values. Viscous fingering (a process by which part of the oil is retained in the well) in Oil Recovery, crack formation in Civil Engineering and the spread of airborne diseases (which bears similarity with the cloud formation process where water vapor is the virus, condensation is the infection process and precipitation is the emission process) in Biology are additional examples. The CRM was integrated with high space resolution using numerical pressures, Jacobi iterations for solving the numerical pressure equations and the fourth-order accurate in time explicit Adams-Bashforth method for solving the evolution equations. In the CRM, the reaction-diffusion parameter ξ for turbulence was set to the Smagorinsky-Lilly model for eddy viscosity and the state equation, condensation rate, radiation and surface temperature were set using the total pressure. With these settings the turbulent wind properly balanced the laminar wind in both case studies - moderate and high Reynolds numbers. The IBM prediction method was tested in this framework with the horizontal laminar wind velocity components and the potential temperature set as control variables, showing that the atmospheric water cycle has higher predictability under this method than under straightforward integrations of the CRM, both for moderate and high Reynolds numbers. The future work may consist in exploring Multigrid methods [7] within a numerical framework where interpolation is efficient, such as spectral elements, to render the iterative CRM pressure solvers more accurate; or else in searching the CRM for control modes of its dynamics (i.e. minimal sets of modes of control variables, such as the horizontal laminar wind velocity components and the potential

temperature, such as the IBM method can suitably predict the evolution of all variables when the remaining unstable modes of the control variables and the turbulent wind velocity components are perturbed); or yet in using robust IBM-driven CRM data to incorporate deterministic ML parameterizations of turbulent processes, i.e. model error, into the anelastic system and then search this reduced CRM system for control modes of its dynamics.

Acknowledgments

The author is indebted with Joe Tribbia for his keen support to this project and gratefully acknowledges the Instituto Nacional de Matemática Pura e Aplicada (IMPA), which is sponsored by CNPq, for providing the necessary computing resources to it. This research did not receive any specific grant from funding agencies in the public, commercial, or not-for-profit sectors.

References

- [1] C. Foias and G. Prodi. “Sur le comportement global des solutions non-stationnaires des équations de Navier-Stokes en dimension 2”. In: **Rend. Sem. Mat. Univ. Padova** 39 (1967), pp. 1–34.
- [2] J. Hadamard. “Les surfaces à courbures opposées et leurs lignes géodésiques”. In: **J. Math. Pures Appl.** 4 (1898), pp. 27–73.
- [3] G. E. Karniadakis, M. Israeli, and S. A. Orszag. “High-order splitting methods for the incompressible Navier-Stokes equations”. In: **J. Computational Physics** 97 (1991), pp. 414–443. DOI: [https://doi.org/10.1016/0021-9991\(91\)90007-8](https://doi.org/10.1016/0021-9991(91)90007-8).
- [4] P. Krause. “Dyson’s split action formula for transport operators”. In: **Matemática Contemporânea** 56:8 (2023), pp. 135–142. DOI: <https://doi.org/10.21711/231766362023/rmc568>.
- [5] P. Krause. “Influence sampling of trailing variables of dynamical systems”. In: **Math. Clim. Weather Forecasting** 3 (2017), pp. 51–63. DOI: <https://doi.org/10.1515/mcwf-2017-0003>.
- [6] P. Krause and J. Tribbia. “Initialization and dynamical stabilization of a cloud-resolving model”. In: **Physics Open** 12 (2022), p. 100117. DOI: <https://doi.org/10.1016/j.physo.2022.100117>.
- [7] R. J. LeVeque. **Finite Difference Methods for Ordinary and Partial Differential Equations: Steady-State and Time-Dependent Problems**. SIAM, 2007. ISBN: 978-0-898716-29-0.
- [8] E. N. Lorenz. “Deterministic nonperiodic flow”. In: **Journal of the Atmospheric Sciences** 20 (1963), pp. 130–141.
- [9] Y. Ogura and N. A. Phillips. “Scale analysis of deep and shallow convection in the Atmosphere”. In: **J. Atmospheric Sciences** 19 (1962), pp. 173–179. DOI: [https://doi.org/10.1175/1520-0469\(1962\)019<0173:SAODAS>2.0.CO;2](https://doi.org/10.1175/1520-0469(1962)019<0173:SAODAS>2.0.CO;2).
- [10] J. Smagorinsky. “General circulation experiments with the primitive equations”. In: **Monthly Weather Review** 91:3 (1963), pp. 99–164. DOI: [https://doi.org/10.1175/1520-0493\(1963\)091<0099:GCEWTP>2.3.CO;2](https://doi.org/10.1175/1520-0493(1963)091<0099:GCEWTP>2.3.CO;2).